Relative Rate and Product Studies of the OH−Acetone Reaction

Jonathan D. Raff, Philip S. Stevens, and Ronald A. Hites*

School of Public and Environmental Affairs, Indiana University, Bloomington, Indiana 47405

Received: January 10, 2005; In Final Form: April 4, 2005

The rate constants for the reaction of acetone (k_H) and d_6-acetone (k_D) with OH radicals have been measured at atmospheric pressure over a range of temperatures by a relative rate method by using on-line mass spectrometry. The following Arrhenius expressions have been determined for these reactions (in units of cm^3 $molecule^{-1}$ s^{-1}): $k_H(T) = (9.84^{+1.55}_{-1.34} \times 10^{-13}) \exp[-(484 \pm 44)/T]$ between 253 and 373 K, and $k_D(T) = (4.05^{+1.27}_{-0.97} \times 10^{-13}) \exp[-(755 \pm 89)/T]$ between 293 and 373 K. This is the first study to investigate the temperature dependence of k_H and k_D by using a relative rate method and confirms previous rate constants determined by absolute methods. Agreement of our rate constants with those determined in the absence of water suggests that the presence of water vapor has a minimal effect on the kinetics of this reaction under the conditions of our study. The observed kinetic isotope effect ($k_H/k_D = 5.6 \pm 0.4$ at 293 K) is evidence that H-atom abstraction occurs in the mechanism. The acetic acid yields of the reaction of OH with acetone and d_6-acetone were also investigated by on-line mass spectrometry. Acetic acid yields show a negative temperature dependence that decreases from 0.12 at 273 K to 0.05 at 353 K. The yields of d_3-acetic acid decrease from 0.20 at 283 K to 0.13 at 323 K. Kinetic modeling of our data suggests that 50−70% of the observed acetic acid in our system may be due to secondary reactions involving acetonoxy and HO_x radical reactions. However, secondary chemistry cannot easily explain the observed formation of d_3-acetic acid in the deuterated system, where about 90% of the observed d_3-acetic acid is likely due to an OH-addition mechanism.

Introduction

Acetone is one of the most abundant organic compounds in the earth's atmosphere with an estimated tropospheric concentration of 0.2−3 ppbv and a global emission of 100 Tg y^{-1}.[1] It is a product of the free radical oxidation of hydrocarbons (e.g., propane, isobutane, and isobutene) and is directly emitted by natural and anthropogenic sources.[1−3] Acetone's atmospheric fate is controlled by direct photolysis,[4−8] reaction with hydroxyl radicals (OH), oxidation by HO_2 radicals,[9] and deposition.[2,10] Acetone is a major source of hydrogen oxide radicals (HO_x) and a precursor of peroxyacetylnitrate (PAN), both of which contribute to the formation of tropospheric ozone.[3,5,11,12] A complete understanding of important tropospheric cycles, therefore, requires an accurate quantification of acetone's loss processes.

The photolysis of acetone has been studied in detail.[4−8] More recently, attention has turned to measuring the rate constant for the reaction of acetone with OH. These studies have employed either pulsed laser-induced fluorescence[13−17] or resonance−fluorescence spectroscopy[14,18] to determine rate constants over a wide range of temperatures. Only one of these studies was carried out at atmospheric pressure.[16]

Relative rate techniques have not been used extensively to investigate the temperature dependence of the OH−acetone reaction. These methods employ straightforward instrumentation and are a convenient way to validate absolute rate measurements. Relative rate measurements also have the advantage of being less sensitive to small amounts of impurities in the reactants and are easily carried out under atmospheric conditions. To date, relative rate constants of the OH−acetone reaction have only been reported for individual temperatures,[19,20] but these measurements do not agree well with rate constants determined by absolute methods.

In this paper, we report our measurements of (a) relative rate constants for the OH−acetone reaction between 253 and 373 K at atmospheric pressure, (b) rate constants of the reaction of OH with d_6-acetone in an effort to study the kinetic isotope effect (KIE), (c) the yield of acetic acid produced by the reaction of acetone and OH between 273 and 353 K, and (d) the yield of d_3-acetic acid from the reaction of d_6-acetone with OH between 283 and 323 K. The contribution of the addition−elimination channel to the overall mechanism has been studied previously. Acetic acid yields as high as 50% have been suggested,[22,23] but all measurements of this yield gave results in the range <1% to <10%.[24−28] This wide discrepancy in the literature warranted further investigation.

Experimental Section

Experimental Procedures. The apparatus we used has been described previously.[29−34] It consists of a 160 or 500 cm^3 quartz reaction chamber mounted in the oven of a Hewlett-Packard 5890 gas chromatograph (for temperature control) and coupled to a Hewlett-Packard 5989A mass spectrometer (operated in the electron ionization mode) via a 75 cm × 100 μm (i.d.) deactivated, fused silica capillary tube (J&W Scientific Inc.). Low temperatures were achieved with cryogenic cooling (liquid N_2) of the GC oven. Reactions were studied with helium (with 20% O_2) as a diluent gas under static conditions at 735−750 Torr. The water content of the gas mixture is estimated (via

* To whom correspondence should be addressed. E-mail: hitesr@indiana.edu.

10.1021/jp0501547 CCC: $30.25
Published on Web 05/10/2005

mass spectrometry) to be $0.1-5 \times 10^{17}$ molecules cm^{-3} over the temperatures studied. OH radicals were produced in situ as follows:

$$O_3 + h\nu\ (\lambda \leq 315\ nm) \rightarrow O(^1D) + O_2 \quad (1)$$

$$O(^1D) + H_2O \rightarrow 2OH \quad (2)$$

Ozone was produced by flowing O_2 through a 12 kV discharge. The stream of O_2/O_3 was combined with a stream of diluent gas that had been bubbled through water at about 291 K and flowed through the reaction chamber for at least 10 min before the chamber was sealed off and the reactants were injected. UV irradiation ($\lambda = 254$ nm) was provided by a single 8 W germicidal lamp (General Electric, G8-T5) attached to the door of the GC oven. We did not observe photodecomposition of acetone under these conditions as verified by monitoring the abundance of acetone ions in the reaction chamber in the absence of the O_3, using on-line mass spectrometry. We also attempted to generate OH by photolyzing a gaseous mixture of hydrogen peroxide. This is a considerably weaker source of OH radicals and could not produce the high OH concentrations required to react with acetone on a reasonable time scale.

Relative Rate Experiments. In a typical experiment, acetone or d_6-acetone vapor (2−10 μL) was injected into the reaction chamber with a gastight syringe (Hamilton Co.). Various amounts of reference compound were subsequently injected to achieve an instrument response approximately identical with that of acetone. The concentration of OH in the reaction chamber was $0.8-5 \times 10^9$ molecules cm^{-3}, as calculated from the known concentration of acetone in the chamber, the previously measured rate constant of acetone,[15] and the decay rate of acetone during the experiment.[32,33]

Derivation of the rate constants is based on the competition of two reactants for a common source of hydroxyl radicals. Assuming the OH reactions are the primary loss processes during UV irradiation of the reaction chamber, the recorded signal intensities for the test and reference compounds follow the relationship,

$$\ln\frac{[\text{test}]_0}{[\text{test}]_t} = \frac{k_{\text{test}}}{k_{\text{ref}}} \ln\frac{[\text{reference}]_0}{[\text{reference}]_t} \quad (3)$$

where the signal intensities are measured at time $t = 0$ and at subsequent times, t. The slope of the plot of $\ln([\text{test}]_0/[\text{test}]_t)$ versus $\ln([\text{reference}]_0/[\text{reference}]_t)$ provides the ratio of the rate constants of the two simultaneous reactions. The independently determined rate constant of the reference compound is multiplied by the value of this ratio to derive the rate constant of the test compound, k_{test}. Previous publications describe in detail how rate constants are derived from raw data.[29−34]

Reference compounds were considered suitable if (a) the selected m/z values from their mass spectra did not overlap with those of the test compound or any background ions, (b) k_{ref} values were of a magnitude such that the ratio of rate constants satisfied the condition $0.1 \leq (k_{\text{test}}/k_{\text{ref}}) \leq 10$, (c) they did not react with O_3, (d) the values of k_{ref} were not pressure dependent, (e) the reaction of OH with the reference compounds did not generate secondary products that reacted with acetone (e.g., Cl or Br), (f) acetone was not a product of the OH−reference compound reactions, (g) the vapor pressures of the reference compounds were adequate over a range of temperatures, and (h) the Arrhenius expressions of the reference compounds were known with sufficient certainty.

Eighteen potential reference compounds were investigated. However, only 1,1-difluoroethane ($C_2H_4F_2$) and difluoromethane (CH_2F_2) were found to be suitable for our system. The m/z values monitored were the following: acetone, 43 ($M - CH_3^+$), 58 (M^+); d_6-acetone, 46 ($M - CD_3^+$); $C_2H_4F_2$, 51 ($M - CH_3^+$), 65 ($M - H^+$); and CH_2F_2, 51 ($M - H^+$). Preliminary experiments were conducted to investigate overlaps in masses from the test and reference compounds according to the experimental approach of Gill and Hites[30] and Khamaganov and Hites.[34] We were unable to measure the molecular ion of d_6-acetone (at m/z 64) due to interferences with what we assume to be oxozone (O_4^+). This species was only produced during the discharge reaction of O_2 and decayed under UV irradiation.

Values of k_{ref} were calculated from the following expressions:

$$k(C_2H_4F_2) = (1.98^{+0.48}_{-0.34} \times 10^{-18})T^2 \times \exp[-(460 \pm 56)/T]\ cm^3\ molecule^{-1}\ s^{-1} \quad (4)$$

$$k(CH_2F_2) = (3.84^{+1.14}_{-0.87} \times 10^{-18})T^2 \times \exp[-(1016 \pm 78)/T]\ cm^3\ molecule^{-1}\ s^{-1} \quad (5)$$

The errors for both equations represent 95% confidence limits and are derived from Atkinson's 1994 recommendation that covered the temperature range of 222−492 and 212−423 K for CH_2F_2 and $C_2H_4F_2$, respectively.[35] Although more recent IUPAC recommendations[36] are available for both compounds, they only cover a limited temperature range (240−300 K) and are not adequate for our work at higher temperatures. Rate constants derived from the older expressions agree well with more recent recommendations in the lower temperature range.

Determination of Acetic Acid Yields. Experiments measuring the acetic acid yield of the OH−acetone reaction were performed by monitoring m/z 58 and 60, the molecular ions of acetone and acetic acid, respectively. Similar to the experiments described above, the reaction vessel was purged with the He/O_2/O_3/H_2O mixture and sealed off. Approximately 0.5 μL of liquid acetone and 0.2 μL of liquid perfluorohexane (the inert internal standard) were injected into either a 160 or 500 cm^3 reaction chamber, and the system was allowed to equilibrate for 10 min before UV irradiation was initiated. The acetic acid molecular ion signal at m/z 60 was corrected for a small background signal, and an eight-point instrumental calibration (using perfluorohexane as the internal standard) was carried out to convert the mass spectrometric signals for acetone and acetic acid into absolute concentrations. Calibration data were collected in separate experiments by measuring the instrumental signal that resulted after injecting known amounts of acetone and acetic acid (solutions in dichloromethane) into the reaction cell in the absence of ozone. A control experiment was performed by injecting acetone into the reaction chamber in the absence of ozone; we did not observe the degradation of acetone or the generation of acetic acid with UV irradiation. An identical procedure was used to determine the yield of d_3-acetic acid (CD_3COOH) from the OH−d_6-acetone reaction. The m/z values 46 and 63 were used to monitor d_6-acetone and d_3-acetic acid, respectively. Poor detection limits at low temperatures and H−D exchange of d_6-acetone at higher temperatures precluded detection of d_3-acetic acid outside the temperature range of 283−323 K. Control experiments in the absence of ozone indicated that photolysis of acetic acid did not occur under the above conditions.

Uncertainties in determining the acetone and acetic acid concentrations arise mostly from errors introduced in preparing the calibration solutions and errors in injection volumes. This

TABLE 1: Summary of Average Measured Rate Constant Ratios, k_{test}/k_{ref}, and Rate Constants k_H and k_D ($\times 10^{-13}$ cm^{-3} molecule^{-1} s^{-1}) for the Reactions of OH with Acetone and d_6-Acetone

T (K)	k_{test}/k_{ref}	k_H or k_D
	acetone vs 1,1-difluoroethane	
253	7.23 ± 1.39[a]	1.49 ± 0.29[a]
263	6.69 ± 0.74	1.60 ± 0.18
273	6.45 ± 0.62	1.77 ± 0.17
283	5.51 ± 0.69	1.72 ± 0.22
293	5.24 ± 0.35	1.86 ± 0.13
303	5.23 ± 0.54	2.08 ± 0.22
308	4.69 ± 0.37	1.98 ± 0.16
313	4.28 ± 0.26	1.92 ± 0.11
323	4.42 ± 0.35	2.20 ± 0.18
333	3.92 ± 0.28	2.17 ± 0.15
343	4.04 ± 0.19	2.46 ± 0.12
373	3.66 ± 0.29	2.94 ± 0.23
	d_6-acetone vs difluoromethane	
293	3.22 ± 0.71	0.332 ± 0.073
303	2.64 ± 0.24	0.326 ± 0.029
313	2.49 ± 0.14	0.365 ± 0.021
323	2.15 ± 0.12	0.371 ± 0.020
333	1.98 ± 0.10	0.400 ± 0.020
343	1.94 ± 0.08	0.455 ± 0.019
353	1.69 ± 0.13	0.454 ± 0.036
373	1.65 ± 0.16	0.580 ± 0.056

[a] The errors represent 95% confidence intervals of the mean.

uncertainty was determined by calculating the yield of acetic acid for one experiment by using calibration curves from three separate calibration solutions, and this uncertainty amounted to a 3% error in the final acetic acid yield. The resulting error is not included in the following discussion. The presence of acetic acid dimer could also lead to errors in yields at lower temperatures. However, we estimate that the dimer concentration was only 8% of the monomer concentration in our experiments at 273 K and rapidly decreased to <1% at temperatures above 298 K. The rate constant of the reaction of OH with the dimer is reported to be 9.2×10^{-15} and 1.1×10^{-13} cm^3 molecule^{-1} s^{-1} at 297 and 326 K, respectively.[37] Therefore, the error in the correction factor that we used to account for the secondary reaction of acetic acid with OH (see below) is expected to be small.

Chemicals. Acetone (>99.9%), d_6-acetone (99.96 atom % D), 1,1-difluoroethane (>98%), difluoromethane (99.7%), acetic acid (99.8%), d_3-acetic acid (99 atom % D), and perfluorohexane (99.9%) were obtained from Aldrich Chemical Co. (Milwaukee, WI) and used without further purification. Ultrahigh purity (99.999%) oxygen and helium were purchased from Praxair, Inc. (Indianapolis, IN).

Results and Discussion

Rate Constant Measurements. The rate constant ratios and rate constants for the reaction of OH with acetone and d_6-acetone at various temperatures are summarized in Table 1. For acetone, the ratios were obtained by averaging the slopes of the relative rate plots for all combinations of acetone and $C_2H_4F_2$ masses. It was only possible to monitor one mass for both d_6-acetone and CH_2F_2, therefore 3−7 experiments were performed to achieve replicate measurements. Uncertainties in the rate constants do not include the error of the reference compound rate constants [estimated at ±20%[35]]. Arrhenius plots of the rate constants for both acetone (k_H) and d_6-acetone (k_D) reactions over the temperature range studied here are shown in Figure 1. The Arrhenius parameters were determined by linear regression of the natural logarithms of the measured rate constants versus

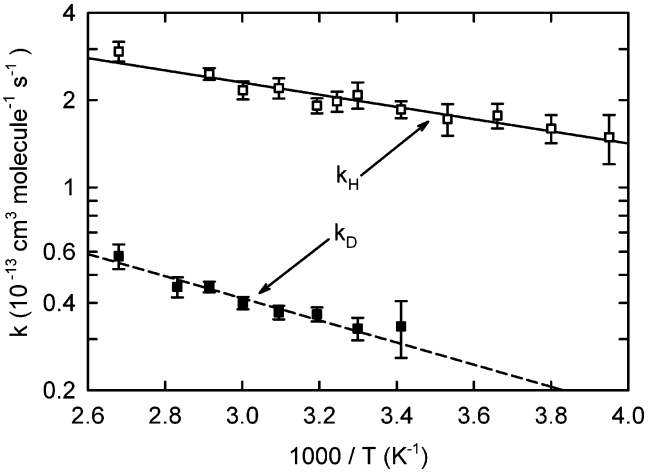

Figure 1. Arrhenius plot of k_H (upper data, open squares) and k_D (lower data, closed squares); Arrhenius parameters are given in eqs 6 and 7 in the text. The error bars represent the 95% confidence limits of the mean. The correlation coefficients (r^2) for the regressions for k_H and k_D are 0.925 and 0.923, respectively.

the corresponding reciprocal absolute temperatures, and the resulting equations are:

$$k_H(T) = (9.84^{+1.55}_{-1.34} \times 10^{-13}) \exp[-(484 \pm 44)/T] \quad (6)$$

$$k_D(T) = (4.05^{+1.27}_{-0.97} \times 10^{-13}) \exp[-(755 \pm 89)/T] \quad (7)$$

where $k_H(T)$ and $k_D(T)$ are valid within the ranges 253−373 and 293−373 K, respectively.

It is important to confirm absolute rate constants in the literature with relative rate techniques because the former are susceptible to errors introduced by reactant impurities. If an impurity effectively competes with acetone for OH in such a system, the rate constant can be artificially high. These effects may be more pronounced at low temperatures if the reaction with an impurity has an inverse temperature dependence. We determined that overlapping ions, which might potentially interfere with the monitored m/z values of acetone and d_6-acetone, were below the detection limit of the mass spectrometer. Therefore, our relative rate constants were not affected by parallel reactions of impurities with OH.

A comparison of k_H over the temperature range 200−500 K reported here and elsewhere is presented in the Arrhenius plot shown in Figure 2. The relative rate constants determined in this work agree well with previously measured data although they are 2−9% higher than previous determinations in the temperature range 298−263 K. The combined data are best fit by the following three-parameter expression, $k_H(T) = 1.24 \times 10^{-13} + (1.14 \times 10^{-11}) \exp(-1575/T)$, between 199 and 498 K. This treatment excludes Kerr and Stocker's rate constant determined at 303 K,[19] which is ~60% higher than other values at similar temperatures.

Figure 3 compares our measurements of k_D to other values in the literature. Fitting the data to a three-parameter expression yields $k_D(T) = 1.87 \times 10^{-14} + (2.81 \times 10^{-11}) \exp(-2363/T)$, between 211 and 498 K. Our measurements agree well with the values of Gierczak et al.[15] and Davis et al.[17] near room temperature. However, at higher temperatures our relative rate constants are approximately 20% lower. Yamada et al.[16] also reported rate constants that were 12−20% lower than those of Gierczak et al. and concluded that systematic errors specific to their measurement apparatus might be responsible for the difference. The Yamada et al. study is also the only report of

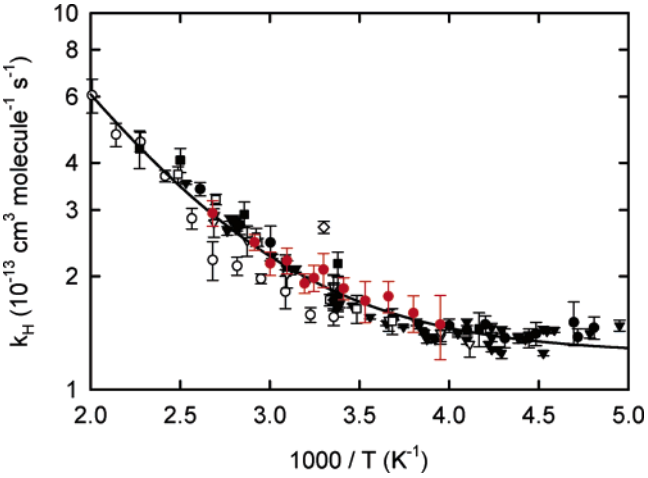

Figure 2. Comparison of k_H determined from our study (red circles) to those of Wallington and Kuryo[18] (squares), Davis et al.[17] (open squares), Gierczak et al.[15] (circles), Yamada et al.[16] (open circles), Wollenhaupt et al.[14] (triangles), Le Calve et al.[13] (open triangles), Kerr and Stocker[19] (open diamond), and Vasvári et al.[23] (diamonds). The best least-squares fit to all data (except the outlier at $1000/T = 3.3$) is $k_H(T) = 1.24 \times 10^{-13} + (1.14 \times 10^{-11}) \exp(-1575/T)$ between 199 and 498 K with an r^2 value of 0.958. The error bars represent the 95% confidence limits of the mean.

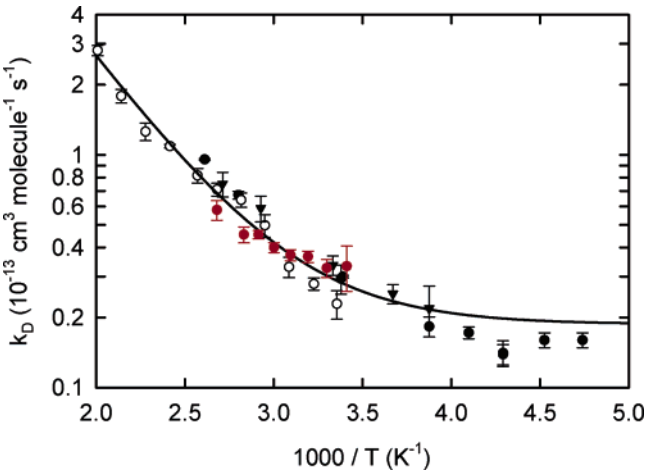

Figure 3. Comparison of k_D determined from our study (red circles) to those of Davis et al.[17] (triangles), Gierczak et al.[15] (circles), and Yamada et al.[16] (open circles). The best least-squares fit to all data is $k_D(T) = 1.87 \times 10^{-14} + (2.81 \times 10^{-11}) \exp(-2363/T)$ between 211 and 498 K with an r^2 value of 0.987. The error bars represent the 95% confidence limits of the mean.

absolute rate measurements made at atmospheric pressure. However, the data of Gierczak et al. do not reveal a noticeable difference in k_D at 295 and 296 K over the pressure range of 25−100 Torr.[15]

The most noticeable feature of Figures 2 and 3 is the curvature in the temperature dependence of k_H and k_D that seems to approach a constant value below 260 K. For acetone, this curvature has been postulated to be due to either a shift in the mechanism from primarily H-abstraction at high temperature to primarily OH-addition at lower temperatures or the formation of a pre-reactive hydrogen-bonded complex with tunneling through the abstraction barrier.[15,16,22,24,26] Unfortunately, we were not able to verify the negative temperature dependence of k_H and k_D observed by others[14,15] at $T < 240$ K due to poor sensitivity and unreasonably slow rates of reaction below 250 K.

Mechanism of the OH−Acetone Reaction. The reaction of acetone with OH may proceed via two parallel channels that include abstraction (eq 8a) and addition−elimination (eq 8b).

$$CH_3C(O)CH_3 + OH \rightarrow CH_3C(O)CH_2^{\bullet} + H_2O \quad (8a)$$

$$CH_3C(O)CH_3 + OH \rightarrow CH_3C(O)OH + CH_3^{\bullet} \quad (8b)$$

It has been suggested that H-atom abstraction from acetone occurs via a doubly hydrogen-bonded reaction complex, while the competing addition−elimination channel proceeds via a chemically activated $(CH_3)_2C(O)OH$ intermediate that dissociates to acetic acid and methyl radical.[23,24,26] Several theoretical studies have concluded that the barrier to OH-addition is substantially higher than that for abstraction, suggesting that acetic acid should be a minor product of the overall reaction.[16,23,24,38,39]

Reports of the actual yield of the acetonyl radical and acetic acid vary widely in the literature. For example, from indirect measurements of CH_3 radicals, Wollenhaupt and Crowley suggested that the acetic acid yield could be as high as 50%;[22] measurements of acetonyl radical yields by Vasvári et al. support this suggestion.[23] However, Vandenberk et al. and Tyndall et al. assigned upper limits of 5% and 10% for acetic acid,[24,25] and Talukdar et al. determined that less than 1% acetic acid was formed between 237 and 353 K, independent of pressure.[26] The latter study also found the acetonyl radical yield to be 96(±11)%, independent of temperature. Using the same experimental technique as Vasvári et al., Turpin et al. determined the branching ratio for acetonyl radical formation to be 0.8−1.0.[27] The same group was unable to detect any acetic acid when they attempted to measure it directly.[28] Although it now seems possible that experimental errors may have led to the low CH_3 and acetonyl radical yields reported previously,[24] the actual yield of acetic acid still remains uncertain. Thus, we studied the mechanism of the OH−acetone reaction by measuring the primary kinetic isotope effect and by directly determining the yield of acetic acid and d_3-acetic acid using on-line mass spectrometry.

Kinetic Isotope Effect. The ratio of the rate constants k_H/k_D calculated from data in Table 1 suggests a primary kinetic isotope effect (KIE). For example, the value of k_H/k_D is 5.6 ± 0.4 at 293 K. Some studies reported that the KIE for acetone/d_6-acetone is inversely dependent on temperature. Recently, Gierczak et al. reported a k_H/k_D of 5.9 ± 0.9 at 298 K and 8.6 ± 0.8 at 212 K.[15] Similarly, if the KIE is calculated from the equations fitted to the data in Figures 2 and 3, we find that it increases from 6.3 ± 0.7 at 298 K to 6.8 ± 1.5 at 212 K. The observed KIE is evidence that a C−H bond breaks during the OH−acetone reaction due to the abstraction of a methyl hydrogen by the OH radical. However, these results do not rule out a significant contribution of reaction 8b if the OH + acetone reaction proceeds through a pre-reactive complex. A larger primary kinetic isotope effect of approximately 12 for the OH + HNO_3 and DNO_3 reactions has been attributed to a hydrogen abstraction mechanism involving the formation of a pre-reactive complex.[40] If the OH + acetone reaction proceeded through a similar mechanism,[26] one might expect a similar primary kinetic isotope effect. The smaller primary kinetic isotope effect observed for the OH + acetone reaction may reflect the contribution of a secondary mechanism to the overall rate constants.[41]

Determination of the Acetic Acid Yield (Φ). We were able to directly observe the concurrent decay of acetone and the

TABLE 2: Measured Yields, Φ, for the Formation of Acetic Acid as a Function of Temperature

T (K)	Φ^a	$\langle\Phi\rangle \pm 2\sigma^b$
273	0.141	0.118 ± 0.056
	0.118	
	0.096	
283	0.130	0.119 ± 0.036
	0.124	
	0.102	
298	0.087	0.082 ± 0.013
	0.082	
	0.077	
298[c]	0.110	0.101 ± 0.019
	0.095	
	0.100	
323	0.072	0.055 ± 0.037
	0.049	
	0.045	
353	0.049	0.047 ± 0.004
	0.046	
	0.046	

[a] Not shown are the associated statistical errors that amount to <0.5% of the absolute yield. [b] The errors represent 95% confidence intervals of the mean. [c] Experiments carried out in the 500 cm^3 reaction chamber; a 160 cm^3 reaction chamber was used for all other experiments.

formation of acetic acid by monitoring the appropriate ions using on-line mass spectrometry. We recently demonstrated the utility of this experimental system for measuring the branching ratios of products resulting from the reaction of isoprene with OH radicals.[42] The acetic acid yield, Φ, is calculated from

$$\Phi = F\frac{[\text{acetic acid}]_t}{[\text{acetone}]_0 - [\text{acetone}]_t} \qquad (9)$$

where F is a correction factor that accounts for the secondary reaction of acetic acid with OH radicals, as described by Atkinson et al.[43] The correction factors were derived by using rate constants for the reaction of OH radicals with acetone (from the fitted equation in Figure 2) and acetic acid,[44] and these factors increase with the extent of the reaction to maxima between 1.2 and 1.7. Plots of the corrected acetic acid concentration against the amount of reacted acetone for all experiments were linear for the first 10−15 min. The average of the slopes derived from the least-squares fit of three experiments at 298 K results in an acetic acid yield of 8.2(±1.3)% and is similar to the upper limits reported by Tyndall et al.[25] However, our yield is higher than that observed by Vandenberk et al.,[24] Talukdar et al.,[26] and Turpin.[28]

The measured yield of acetic acid shows a negative temperature dependence between 273 and 353 K; see Table 2. The linear regression of acetic acid yields versus temperature, shown in Figure 4, is significant at the 95% confidence level. Such behavior is consistent with an addition mechanism involving the formation of an intermediate complex,[14] but suggests that the barrier to OH-addition is lower than theoretical predictions.[24,38] The opposite trend was observed by Wollenhaupt and Crowley, who inferred acetic acid yields of 0.50 and 0.33 at 298 and 233 K, respectively, based on their determination of trapped CH_3.[22]

The branching ratio for deuterated acetic acid from the reaction of OH with d_6-acetone,

$$CD_3C(O)CD_3 + OH \rightarrow CD_3C(O)CD_2^{\bullet} + DOH \qquad (10a)$$

$$CD_3C(O)CD_3 + OH \rightarrow CD_3C(O)OH + CD_3^{\bullet} \qquad (10b)$$

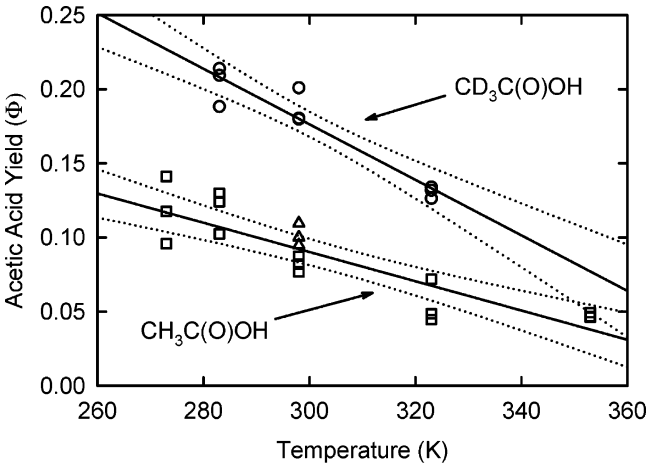

Figure 4. Acetic acid (squares and triangles) and d_3-acetic acid (circles) yields at various temperatures. Shown are experiments carried out in 160 cm^3 (squares and circles) and 500 cm^3 (triangles) reaction chambers. Solid lines are the linear fit to each data set ($r^2 = 0.774$ and 0.718 for acetic acid and d_3-acetic acid, respectively). The dotted lines represent the 95% confidence limit of the fits.

TABLE 3: Measured Yields, Φ, and Average Rate Constants, k_{add} ($\times 10^{-14}$ cm^{-3} $molecule^{-1}$ s^{-1}), for the Formation of d_3-Acetic Acid as a Function of Temperature

T (K)	Φ^a	$\langle\Phi\rangle \pm 2\sigma^b$	$k_{add} \pm 2\sigma^b$
283	0.188	0.204 ± 0.034	$0.572^{+0.460}_{-0.255}$
	0.214		
	0.209		
298	0.201	0.187 ± 0.030	$0.600^{+0.466}_{-0.262}$
	0.180		
	0.180		
323	0.134	0.131 ± 0.010	$0.511^{+0.375}_{-0.216}$
	0.132		
	0.126		

[a] Not shown are the associated statistical errors that amount to <0.5% of the absolute yield. [b] The errors represent 95% confidence intervals of the mean.

was found to increase from 0.13 to 0.2 between 323 and 283 K; see Table 3. As shown in Figure 4, the absolute yields of d_3-acetic acid are higher than those of acetic acid. This is not surprising because the OH-addition channel is expected to play a more important role in the deuterated system since the barrier for D-abstraction is higher than that for H-abstraction. Our measurements of acetic acid and d_3-acetic acid yields suggest that, although hydrogen abstraction dominates the overall reaction mechanism, an addition mechanism may be more significant than previously thought. However, the present system is more complex than some previous studies done at low pressures in the absence of O_2 and H_2O, and it is possible that other mechanisms exist for the formation of acetic acid.

The Role of Water in the Acetone−OH Mechanism. The works of Vandenberk et al.[24] and Talukdar et al.[26] are the only studies that determined acetic acid yields from detectable amounts of acetic acid generated from reaction 8. The yields of the latter study were significantly lower than ours and were constant between 237 and 353 K. Unlike our experiments, these studies were carried out at low pressure in the absence of water. Recent theoretical work by Canneaux and co-workers[45] suggests that water could catalytically enhance the rate of the OH−acetone reaction, forming hydrogen-bonded complexes and transition states [e.g., $(CH_3)_2CO\cdots H_2O\cdots HO$] for both the abstraction and addition channels. These water complexes were shown to significantly reduce the activation energies for both

hydrogen abstraction and OH addition relative to the water-free system.[45] Thus, it is possible that the higher acetic acid yields observed in this study are due to an enhancement of this channel in the presence of water. However, our overall rate constants are not significantly different from those measured previously under water-free conditions. Furthermore, the theoretical study mentioned above predicts that the abstraction channel should still be the predominant channel despite any rate enhancement of reaction 8.[45]

Canneaux and co-workers calculated equilibrium constants for the formation of termolecular $(CH_3)_2CO\cdots H_2O\cdots HO$ complexes and suggested that such complexes may be important under certain laboratory conditions.[45] Using their equilibrium constant for the formation of the termolecular OH−addition complex ($K_{add}(298\ K) = 1.14 \times 10^{-41}$ cm^6 molecule^{-2}) and concentrations typical of our product studies ([acetone] $\approx 2 \times 10^{16}$ molecule cm^{-3}, [H_2O] $\approx 5 \times 10^{17}$ molecule cm^{-3}, and [OH] $\approx 5 \times 10^9$ molecule cm^{-3}), we estimate that the $(CH_3)_2CO\cdots H_2O\cdots HO$ complexes for the addition pathway may be present at concentrations of $\sim 5 \times 10^2$ molecule cm^{-3} in our room-temperature experiments. The concentration of termolecular abstraction complexes ($K_{abs}(298\ K) = 4.72 \times 10^{-41}$ cm^6 molecule^{-2})[45] would be of the same order of magnitude. These concentrations would not change appreciably at lower temperatures since any shift of the equilibrium to complex formation at lower temperatures is accompanied by a decrease in the concentration of water in the gas phase. These theoretical results suggest that concentrations of $(CH_3)_2CO\cdots H_2O\cdots HO$ complexes are likely to be insignificant and suggest that water should not play a major role in the gas-phase kinetics of our system. However, additional measurements of the potential water dependence of the kinetics of the OH + acetone reaction are needed to confirm these results.

Heterogeneous Reactions. The small reaction chambers used in our experiments help to increase the sensitivity of our system for semivolatile organic compounds. The disadvantage, however, is that heterogeneous reactions on the wall surfaces might interfere with our experiments. To investigate this possibility, we performed acetic acid yield measurements in quartz reaction chambers of two different volumes, 160 and 500 cm^3. The larger reaction chamber has approximately twice the surface area of the smaller chamber and both were charged with the same amount of acetone (i.e., the initial concentration of acetone in the larger chamber was approximately half of that used in the smaller chamber). Using the larger reaction cell, we did not observe a notable difference in the acetic acid yields measured at 298 K; see Table 2 and Figure 4. We conclude that wall effects are insignificant (at least at room temperature) or that our method is not sensitive enough to distinguish between differences in yield caused by the change in surface area of the reaction chambers.

Secondary Reactions. It is possible that acetic acid is formed as a product of secondary reactions of acetonyl radicals. Acetonyl radicals produced from reaction 8a undergo rapid reaction with O_2 ($k_{298} = 7.5 \times 10^{-11}$ cm^3 molecule^{-1} s^{-1}) to form acetonyl peroxy radicals.[46] The latter undergo self-reaction to form acetonoxy radicals that in turn rapidly decompose to acetyl radicals and CH_2O.[46]

$$CH_3C(O)CH_2 + O_2 + M \rightarrow CH_3C(O)CH_2O_2 + M^* \quad (11)$$

$$2CH_3C(O)CH_2O_2 \rightarrow 2CH_3C(O)CH_2O + O_2 \quad (12)$$

$$CH_3C(O)CH_2O \rightarrow CH_3C(O) + CH_2O \quad (13)$$

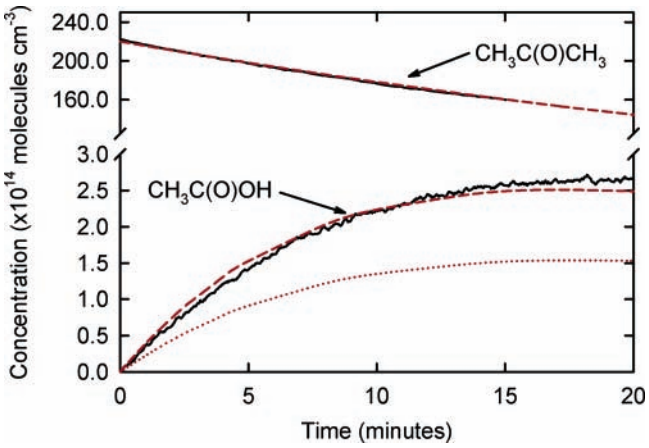

Figure 5. Experimental (solid black lines) and modeled (dashed red lines) concentration profiles of the OH radical-initiated oxidation of acetone and formation of acetic acid at 298 K and 740 Torr. Contributions of secondary reactions to the modeled acetic acid concentrations are represented by the dotted line.

The acetyl radicals produced in this sequence could subsequently react with excess O_2 to form acetyl peroxy radicals ($k_{298} = 5 \times 10^{-11}$ cm^3 molecule^{-1} s^{-1}), which in turn would react with HO_2 to form peracetic and acetic acids with a branching ratio, k_{15a}/k_{15}, of ~ 0.7.[46]

$$CH_3C(O) + O_2 + M \rightarrow CH_3C(O)O_2 + M^* \quad (14)$$

$$CH_3C(O)O_2 + HO_2 \rightarrow CH_3C(O)O_2H + O_2 \quad (15a)$$

$$\rightarrow CH_3C(O)OH + O_3 \quad (15b)$$

Acetic acid may also be generated in the reaction of acetyl peroxy radicals with methyl peroxy or acetonyl peroxy radicals.[47,48] The rate of the reaction of acetyl peroxy radicals with HO_2 shows a negative temperature dependence,[49,50] while k_{15a}/k_{15b} decreases with decreasing temperature.[46,47,50] This trend is consistent with the acetic acid-forming channel in our system. Furthermore, Orlando et al. reported that acetic acid is formed from the degradation of acetonyl radicals produced from the reaction of acetone and Cl in the presence of O_2.[46]

To evaluate these pathways, we created a model of the temporal profile of acetone and acetic acid using some of the mechanisms from the study of Orlando et al.,[46] including self-reactions of HO_x radicals. The simulations were able to reproduce the observed acetone and acetic acid concentration profiles despite the large uncertainty in the reaction rates of some of the mechanisms involved. Figure 5 compares the modeled acetone and acetic acid concentrations to our experimental results. The dotted line in Figure 5 is the maximum amount of acetic acid formed if secondary reactions were the only source of acetic acid in our system. These results indicate that a significant amount (ca. 50−70% of the overall yield) of the acetic acid may be due to secondary reactions of acetonyl radical produced in reaction 8a. This suggests that the actual yield of acetic acid formed via reaction 8b is lower than the overall acetic acid yields in Table 2 and may be 0.03−0.05 at 298 K, in much closer agreement with previous findings.[24,25] Moreover, if secondary chemistry were primarily responsible for the observed yields of acetic acid in these experiments, the observed yield of d_3-acetic acid would be significantly smaller because there are fewer secondary reactions that could lead to the production of CD_3COOH.

To further investigate the deuterated system, a model was created including rate constants for the OH−d_6-acetone reaction

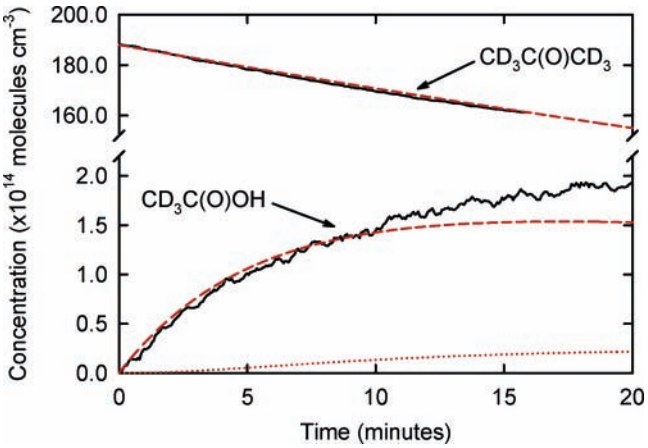

Figure 6. Experimental (solid black lines) and modeled (dashed red lines) concentration profiles of the OH radical-initiated oxidation of d_6-acetone and formation of d_3-acetic acid at 298 K and 740 Torr. Contributions of secondary reactions to the modeled d_3-acetic acid concentrations are represented by the dotted line.

determined in this study and by assuming only minor differences in the kinetics of protiated and deuterated species involved in the secondary reactions discussed above. Results of the model, including the contribution of secondary reaction, are compared to our measurements in Figure 6. In this case, reaction 10b predominates and secondary reactions are only able to account for less than 10% of the observed concentrations of d_3-acetic acid. The most likely route to d_3-acetic acid via secondary reactions is an analogue of reaction 15b involving the reaction of deuterated acetyl peroxy radicals with HO_2

$$CD_3C(O)O_2 + HO_2 \rightarrow CD_3C(O)OH + O_3 \qquad (16)$$

The pronounced difference in contributing factors to acetic acid and d_3-acetic acid yields in the two systems emphasizes the importance of the initial abstraction step (reactions 8a and 10a) as the rate-determining step that generates the acetonyl (and d_5-acetonyl) radicals necessary to drive the secondary reactions. As a consequence, the amount of acetic acid produced via secondary reactions is expected to be greatest in regions of the atmosphere where acetonyl radical levels are highest.

Knowing that secondary reactions contribute only minimally to the observed yield of d_3-acetic acid, we may assume that reactions 10a and 10b are the only channels responsible for the observed loss of d_6-acetone in the presence of OH. The values of the formation constants, k_{add}, for d_3-acetic acid are then derived by multiplying the d_3-acetic acid yields in Table 3 by the k_D values from eq 7. The rate constants for this pathway are listed in Table 3 and are described by the Arrhenius equation

$$k_{add}(T) = (2.2^{+2.8}_{-1.2} \times 10^{-15}) \exp[(285 \pm 246)/T) \qquad (17)$$

between 283 and 323 K. The large errors associated with this expression make it difficult to predict the behavior of this channel at lower temperatures. However, such a negative temperature dependence of the d_3-acetic acid yields may explain the non-Arrhenius temperature dependence observed in the measured rate constants of k_D between 298 and 211 as shown in Figure 3.

Given that the formation of acetic acid through an addition channel is unlikely to have a significant isotope effect, the observed rate of d_3-acetic acid formation likely reflects the overall rate of acetic acid formation through reaction 8b. Based on the observed rates for the OH−acetone reaction, this rate would correspond to a yield of acetic acid of approximately 3% at room temperature, consistent with previous measurements of this yield and the kinetic modeling studies discussed above. However, the observed negative temperature dependence for this channel is in contrast to theoretical predictions.[24,38] For example, using the CBS-RAD(B,B) multilevel energy method, Masgrau et al. found the branching ratio for the addition−elimination mechanism to increase from 0.12 to 1.68%, as the temperature increased from 150 to 1500 K.[38] Additional measurements of the temperature dependence of the acetic acid yield are needed to resolve this discrepancy.

Acknowledgment. We thank Dr. Maxine Davis for helpful discussions. This work was supported by a grant from the Atmospheric Chemistry section of the National Science Foundation (Grant ATM-0106705).

References and Notes

(1) Jacob, D. J.; Field, B. D.; Jin, E. M.; Bey, I.; Li, Q.; Logan, J. A.; Yantosca, R. M.; Singh, H. B. *J. Geophys. Res.* **2002**, *107*, 4100; doi 10.1029/2001JD000694.

(2) Singh, H. B.; O'Hara, D. O.; Herlth, D.; Sachse, W.; Blake, D. R.; Bradshaw, J. D.; Kanakidou, M.; Crutzen, P. J. *J. Geophys. Res.* **1994**, *99*, 1805−1819.

(3) Singh, H. B.; Kanakidou, M.; Crutzen, P. J.; Jacob, D. J. *Nature* **1995**, *378*, 50−54.

(4) Gardner, E. P.; Wijayaratne, R. D.; Calvert, J. G. *J. Phys. Chem.* **1984**, *88*, 5069−5076.

(5) McKeen, S. A.; Gierczak, T.; Burkholder, J. B.; Wennberg, P. O.; Hanisco, T. F.; Keim, E. R.; Gao, R.-S.; Liu, S. C.; Ravishankara, A. R.; Fahey, D. W. *Geophys. Res. Lett.* **1997**, *24*, 3177−3180.

(6) Gierczak, T.; Burkholder, J. B.; Bauerle, S.; Ravishankara, A. R. *Chem. Phys.* **1998**, *231*, 229−244.

(7) Warneck, P. *Atmos. Environ.* **2001**, *35*, 5773−5777.

(8) Blitz, M. A.; Heard, D. E.; Pilling, M. J.; Arnold, S. R.; Chipperfield, M. P. *Geophys. Res. Lett.* **2004**, *31*, L06111.

(9) Hermans, I.; Nguyen, T. L.; Jacobs, P. A.; Peeters, J. *J. Am. Chem. Soc.* **2004**, *126*, 9908−9909.

(10) Chatfield, R. B.; Gardner, E. P.; Calvert, J. G. *J. Geophys. Res.* **1987**, *92*, 4208−4216.

(11) Jaeglé, L.; Jacob, D. J.; Brune, W. H.; Wennberg, P. O. *Atmos. Environ.* **2001**, *35*, 469−489.

(12) Wennberg, P. O.; Hanisco, T. F.; Jaegle, L.; Jacob, D. J.; Hintsa, E. J.; Lanzendorf, E. J.; Anderson, J. G.; Gao, R.-S.; Keim, E. R.; Donnelly, S. G.; Del Negro, L. A.; Fahey, D. W.; McKeen, S. A.; Salawitch, R. J.; Webster, C. R.; May, R. D.; Herman, R. L.; Proffitt, M. H.; Margitan, J. J.; Atlas, E. L.; Schauffler, S. M.; Flocke, F.; McElroy, C. T.; Bui, T. P. *Science* **1998**, *279*, 49−53.

(13) Le Calvé, S.; Hitier, D.; Le Bras, G.; Mellouki, A. *J. Phys. Chem. A* **1998**, *102*, 4579−4584.

(14) Wollenhaupt, M.; Carl, S. A.; Horowitz, A.; Crowley, J. N. *J. Phys. Chem. A* **2000**, *104*, 2695−2705.

(15) Gierczak, T.; Gilles, M. K.; Bauerle, S.; Ravishankara, A. R. *J. Phys. Chem. A* **2003**, *107*, 5014−5020.

(16) Yamada, T.; Taylor, P. H.; Goumri, A.; Marshall, P. *J. Chem. Phys.* **2003**, *119*, 10600−10606.

(17) Davis, M.; Drake, W.; Vimal, D.; Stevens, P. *J. Photochem. Photobiol. A: Chem.* To be submitted for publication.

(18) Wallington, T. J.; Kurylo, M. J. *J. Phys. Chem.* **1987**, *91*, 5050−5054.

(19) Kerr, J. A.; Stocker, D. W. *J. Atmos. Chem.* **1986**, *4*, 253−262.

(20) Cox, R. A.; Derwent, R. G.; Williams, M. R. *Environ. Sci. Technol.* **1980**, *14*, 57−61.

(21) Chiorboli, C.; Bignozzi, C. A.; Maldotti, A.; Giardini, P. F.; Rossi, A.; Carassiti, V. *Int. J. Chem. Kinet.* **1983**, *15*, 579−586.

(22) Wollenhaupt, M.; Crowley, J. N. *J. Phys. Chem. A* **2000**, *104*, 6429−6438.

(23) Vasvári, G.; Szilágyi, I.; Bencsura, Á.; Dóbé, S.; Bérces, T.; Henon, E.; Canneaux, S.; Bohr, F. *Phys. Chem. Chem. Phys.* **2001**, *3*, 551−555.

(24) Vandenberk, S.; Vereecken, L.; Peeters, J. *Phys. Chem. Chem. Phys.* **2002**, *4*, 461−466.

(25) Tyndall, G. S.; Orlando, J. J.; Wallington, T. J.; Hurley, M. D.; Goto, M.; Kawasaki, M. *Phys. Chem. Chem. Phys.* **2002**, *4*, 2189−2193.

(26) Talukdar, R. K.; Gierczak, T.; McCabe, D. C.; Ravishankara, A. R. *J. Phys. Chem. A* **2003**, *107*, 5021−5032.

(27) Turpin, E.; Fittschen, C.; Tomas, A.; Devolder, P. *J. Atmos. Chem.* **2003**, *46*, 1−13.

(28) Turpin, E., Ph.D. Dissertation, Université de Sciences et Technologies de Lille, December 2004.
(29) Lee, W.; Stevens, P. S.; Hites, R. A. *J. Phys. Chem. A* **2003**, *107*, 6603−6608.
(30) Gill, K. J.; Hites, R. A. *J. Phys. Chem. A* **2002**, *106*, 2538−2544.
(31) Anderson, P. N.; Hites, R. A. *Environ. Sci. Technol.* **1996**, *30*, 301−306.
(32) Anderson, P. N.; Hites, R. A. *Environ. Sci. Technol.* **1996**, *30*, 1756−1763
(33) Brubaker, W. W.; Hites, R. A. *J. Phys. Chem. A* **1998**, *102*, 915−921.
(34) Khamaganov, V. G.; Hites, R. A. *J. Phys. Chem. A* **2001**, *105*, 815−822.
(35) Atkinson, R. *J. Phys. Chem. Ref. Data Monogr.* **1994**, *2*, 1−216.
(36) Atkinson, R.; Baulch, D. L.; Cox, R. A.; Crowley, J. N.; Hampson, R. F.; Kerr, J. A.; Rossi, M. J.; Troe, J. *Summary of Evaluated Kinetic and Photochemical Data for Atmospheric Chemistry*, 2004. Available online at: http://www.iupac-kinetic.ch.cam.ac.uk/.
(37) Singleton, D. L.; Paraskevopoulos, G.; Irwin, R. S. *J. Am. Chem. Soc.* **1989**, *111*, 5248−5251.
(38) Masgrau, L.; González-Lafont, À.; Lluch, J. M. *J. Phys. Chem. A* **2002**, *106*, 11760−11770.
(39) Henon, E.; Canneaux, S.; Bohr, F.; Dóbé, S. *Phys. Chem. Chem. Phys*. **2003**, *5*, 333−341.
(40) Brown, S. S.; Burkholder, J. B.; Talukdar, R. K.; Ravishankara, A. R. *J. Phys. Chem. A* **2002**, *105*, 1605−1614.
(41) Farkas, E.; Szilágyi, I.; Dóbé, S.; Bérces, T.; Márta F. *React. Kinet. Catal. Lett.* **2003**, *80*, 351−358.
(42) Lee, W.; Baasandorj, M.; Stevens, P.; Hites, R. A. *Environ. Sci. Technol.* **2005**, *39*, 1030−1036.
(43) Atkinson, R.; Aschmann, S. M.; Carter, W. P. L.; Winer, A. M.; Pitts, J. N. *J. Phys. Chem.* **1982**, *86*, 4563−4569.
(44) Butkovskaya, N. I.; Kukui, A.; Pouvesle, N.; Le Bras, G. *J. Phys. Chem. A* **2004**, *108*, 7021−7026.
(45) Canneaux, S.; Sokolowski-Gomez, N.; Henon, E.; Bohr, F.; Dóbé, S. *Phys. Chem. Chem. Phys*. **2004**, *6*, 5172−5177.
(46) Orlando, J. J.; Tyndall, G. S.; Vereecken, L.; Peeters, J. *J. Phys. Chem. A* **2000**, *104*, 11578−11588.
(47) Horie, O.; Moortgat, G. K. *J. Chem. Soc., Faraday Trans.* **1992**, *88*, 3305−3312.
(48) Bridier, I.; Veyret, B.; Lesclaux, R.; Jenkin, M. E. *J. Chem. Soc., Faraday Trans.* **1993**, *89*, 2993−2997.
(49) Moortgat, G. K.; Veyret, B.; Lesclaux, R. *Chem. Phys. Lett.* **1989**, *160*, 443−447.
(50) Crawford, M. A.; Wallington, T. J.; Szente, J. J.; Maricq, M. M.; Francisco, J. S. *J. Phys. Chem. A* **1999**, *103*, 365−378.